

An evaluation of high-throughput approaches to QTL mapping in *S. cerevisiae*

Wilkening S.*¹, Lin G.*¹, Fritsch E.S.*¹, Tekkedil M.M.*¹, Anders S.*¹, Kuehn R. §¹, Nguyen M. §¹, Aiyar R.S.*¹, Proctor M. §¹, Sakhanenko N.A. †², Galas D.J. †,‡², Gagneur J.*¹, Deutschbauer A. **¹, Steinmetz L.M.*^{1,§,2}

*European Molecular Biology Laboratory, Genome Biology Unit, Meyerhofstrasse 1, 69117 Heidelberg, Germany. §Stanford Genome Technology Center, 855 S. California Avenue, Palo Alto, CA 94304, USA. †Pacific Northwest Diabetes Research Institute, 720 Broadway, Seattle, WA 98122, USA. ‡Luxembourg Centre for Systems Biomedicine, University of Luxembourg, 7, Avenue des Hauts-Fourneaux, L-4362, Esch-sur-Alzette, Luxembourg. **Physical Biosciences Division, Lawrence Berkeley National Laboratory, 1 Cyclotron Road, Mailstop 977-152, Berkeley, California 94720, USA.

Raw sequence files can be downloaded from the Sequence Read Archive (SRA) (submission no. ERP002467): <http://www.ncbi.nlm.nih.gov/sra>

¹These authors contributed equally to this work.

²Corresponding author: Meyerhofstr. 1, 69117 Heidelberg, E-mail: lars.steinmetz@embl.de

Running title: High-throughput QTL mapping approaches

Key words: QTL mapping, bulk segregant analysis, individual segregant analysis, next generation sequencing, yeast, reciprocal hemizygosity scanning

Abstract

Dissecting the molecular basis of quantitative traits is a significant challenge, and is essential for understanding complex diseases. Even in model organisms, precisely determining causative genes and their interactions has remained elusive, due in part to difficulty in narrowing intervals to single genes, and in detecting epistasis or linked quantitative trait loci. These difficulties are exacerbated by limitations in experimental design, such as low numbers of analyzed individuals, and polymorphisms between parental genomes. We address these challenges by applying three independent high-throughput approaches for QTL mapping to map the genetic variants underlying eleven phenotypes in two genetically distant *Saccharomyces cerevisiae* strains, namely: 1) individual analysis of over 700 meiotic segregants, 2) bulk segregant analysis, and 3) reciprocal hemizygosity analysis, a new genome-wide method we developed. We identified differences in the performance of each approach and, by combining them, identified eight polymorphic genes that affect eight different phenotypes: colony shape, flocculation, growth on non-fermentable carbon sources, and resistance to drugs, salt, and heat. Our results demonstrate the power of individual segregant analysis to dissect quantitative trait loci and address the underestimated contribution of interactions between variants. We also reveal confounding factors like mutations and aneuploidy in pooled approaches, providing valuable lessons for future designs of complex trait mapping studies.

Introduction

Most medical and agricultural traits are complex, influenced by multiple alleles with different effect sizes that interact to produce inherited phenotypic variation. Previous studies in model organisms (STEINMETZ and DAVIS 2004; EHRENREICH *et al.* 2009; FLINT and MACKAY 2009; FLINT 2011) have yielded insights into genetic principles that shape complex traits. These studies have shown that besides major quantitative trait loci (QTLs) with large effects, many loci with smaller effects contribute to phenotypic variation. Indeed, although many alleles have been associated with complex traits in humans, their individual and cumulative effects are usually small (<10%) (LANGO ALLEN *et al.* 2010). Further studies have revealed extensive context-dependent effects such as epistasis or genotype-by-sex interactions, as well as pleiotropic effects, most instances of which have likely not been detected. Hence understanding the genetic basis of complex traits remains an open challenge (STRANGER *et al.* 2011).

In this study, we applied three high-throughput methods for the first time to comprehensively identify causative variants underlying eleven phenotypes in two genetically distant yeast strains, S96 and SK1 (LITI *et al.* 2009; SCHACHERER *et al.* 2009). Each method begins with a hybrid generated by crossing these two strains. The first method is the commonly used Bulk Segregant Analysis (BSA) (SEGRE *et al.* 2006; BIRKELAND *et al.* 2010; EHRENREICH *et al.* 2010; WENGER *et al.* 2010; PARTS *et al.* 2011; SWINNEN *et al.* 2012), in which, millions of segregants from the hybrid undergo selection under an environmental pressure. Quantitative trait locus (QTL) mapping is then performed by identifying regions of allelic enrichment via sequencing of the pool (Figure 1).

The second method utilized here is Individual Segregant Analysis (ISA) of 720 segregants from the hybrid. These segregants were genotyped by next-generation sequencing (WILKENING *et al.* 2013) and individually phenotyped to detect genomic regions linked to the phenotypes of interest (Figure 1). Most previous QTL mapping studies in yeast have been performed with sample sizes on the order of 100 segregants and up to 3000 markers (average SNP distance: 4 kb) (STEINMETZ *et al.* 2002; BREM *et al.* 2005; GATBONTON *et al.* 2006; Foss *et al.* 2007; Hu *et al.* 2007; MARULLO *et al.* 2007; NOGAMI *et al.* 2007; PERLSTEIN *et al.* 2007; EHRENREICH *et al.*

2009; LI *et al.* 2013). Our experiment thus increases the sample size by 7-fold and the number of markers by 20-fold (average SNP distance: 150 bp). To date, only one study with a similar number of segregants (1008) has been published; however, it did not detect causative genes (Bloom *et al.* 2013).

To attain QTL mapping at single-gene resolution, we developed and applied a third method termed Reciprocal Hemizygosity Scanning (RHS). For this method, we constructed a hemizygous deletion collection in the hybrid by deleting either the SK1 or the S96 allele and replacing it with a kanamycin resistance gene (KanMX) and a molecular barcode (Figure 1) (WINZELER 1999). This collection includes ~75% of the open reading frames (ORFs) in the yeast genome, allowing for the direct comparison of allelic variants within a single pooled experiment on a genome-wide scale (STEINMETZ *et al.* 2002; STEINMETZ and DAVIS 2004). This is the first report of this genome-wide approach including more than 19,000 hemizygous strains (~4,861 genes deleted in duplicate per background).

Overlaying QTLs detected by these three methods yielded extremely high resolution, allowing us to identify the putative allelic variants underlying eight phenotypes. We also discovered strong interactions between QTLs and differences between the three approaches, which can partially be explained by different experimental parameters (e.g. period of growth), but also by confounding factors such as accumulation of mutations influencing the pooled RHS and BSA approaches.

Materials and Methods

Yeast strain generation

Haploid strains from S288c (BY4742 prototrophic *MATalpha*, referred to as “S96”) and SK1 (SK1 *MATa ura3Δ his3Δ flo8Δ can1Δ::STE2pr-HIS3*) were crossed and an individual hybrid strain was sporulated by transferring the cells grown in YPD (Yeast Extract 10g/L, Bacto Peptone 20g/l, Dextrose 20g/L) to 200ml sporulation medium (0.5% (w/v) potassium acetate) and incubating them at 22°C with agitation. After spreading the cells on YPD plates, 768 clones were randomly picked in eight 96-well

plates, grown overnight, and stored as glycerol stocks. This set of segregants can be copied and sent to other labs upon request. For BSA, we crossed our haploid SK1 strain, in which the *PMS1* open reading frame was exchanged with its S288c version to make it more genetically stable (HECK *et al.* 2006; DEMOGINES *et al.* 2008b) (SK1 *MATa ura3Δ his3Δ flo8Δ can1Δ::STE2pr-HIS3 PMS1[S288c]*), with an S96 strain (BY4742 *MATalpha ura3Δ his3Δ can1Δ::STE2pr-HIS3*). Two independent crosses were grown in 100ml YPD until $OD_{600nm} = 1$ and sporulated as described above. We used the Synthetic Genetic Array (SGA) marker system to select for *MATa* strains on SD plates lacking histidine and supplemented with L-canavanine (60mg/ml) (TONG *et al.* 2001; PAN *et al.* 2004). The resulting colonies were scraped off the plates with an estimated number of 4×10^8 independent segregants per pool. Aliquots of the pool were frozen at -80°C in 15% glycerol for later use. *ENA6* was amplified from genomic DNA of SK1 and cloned into the p416 expression vector (MUMBERG *et al.* 1995) using *Spel* and *Xhol* restriction sites (Table S1). The empty plasmid as well as the *ENA6*-containing plasmid were transformed into SK1 cells and tested in normal and high salt conditions.

Genotyping

Both ISA and BSA analyses were performed with the same 65,234 single nucleotide polymorphisms (SNP) positions, as described before (WILKENING *et al.* 2013). In brief, sequences were aligned to the S288c reference genome (SGD), using Novoalign and only allowing unique alignments. Realignment of the subsequent BAM files, SNP calling and genotyping were performed using GATK (McKENNA *et al.* 2010). For ISA segregants, missing genotypes were imputed with BEAGLE (BROWNING and BROWNING 2007). In total, 768 segregants were sequenced, but from the coverage, aneuploidies were detected in 26 individual segregants (WILKENING *et al.* 2013). After exclusion of these aneuploid strains, strains with low coverage or contamination, 720 segregants were used for subsequent analyses.

QTL mapping

For ISA, we estimated the genetic map for our dataset and calculated the LOD score at each position using R/qtl (BROMAN *et al.* 2003). The threshold at 5% significance level was estimated using the permutation test implemented in R/qtl.

To identify smaller effect QTLs and interactions between QTLs for the high salt and high temperature phenotypes, we stratified the ISA samples according to the major QTL allele prior to repeating QTL analysis. In principle this is similar to using the genotypes at major QTLs as a covariate, as described in previous studies (Broman 2001). For BSA the allele frequency was calculated at each SNP position for all conditions. The allele frequency was fitted using local polynomial regression assuming binomial distribution and confidence intervals were called using a bootstrapping method. To determine whether the allele frequency at the peak for a given condition was significant compared to the control (YPD 30°C, 100 generations), a permutation test was performed for each peak and p-values were corrected using Benjamini-Hochberg (details in Supplementary Notes).

We also performed an *in silico* comparison of the ISA method with a simulated BSA using only the best performing strains (pool of 50 segregants with extreme phenotypes) for eight of the phenotypes analyzed in this study (Figure S1).

Estimating heritability of traits

A genomic selection method was used to estimate, for each trait, the proportion of phenotypic variance that could be explained by using all the 65,234 markers used for QTL mapping. Ridge regression best linear unbiased prediction (rrBLUP) was applied using the rrBLUP package (ENDELMAN 2011). The model has two components of error, genetic variance (V_g) and error variance (V_e). The heritability of the trait, which is the proportion of phenotypic variance that can be explained by all genetic markers, can be estimated by calculating $V_g / (V_g + V_e)$. For estimating narrow sense heritability, the additive kinship matrix described in the rrBLUP package was used as the relationship matrix, and for estimating broad sense heritability, the non-additive Gaussian kernel was used.

Phenotyping

For ISA, individual strains were phenotyped in 96 well plates by growth curve analysis (PROCTOR *et al.* 2011). Cells were grown overnight in YPD to saturation to obtain similar densities for all strains. These colonies were replicated in the medium of interest in transparent 96-well plates and grown until saturation (usually 1-2 days). Doubling times were calculated from OD measurement of liquid cultures at a wavelength of 595nm in a plate reader (Genios, Tecan) as previously described (ST

ONGE *et al.* 2007). The relative fitness was calculated as (1/doubling time at stress condition)/(1/doubling time in YPD at 30°C). The phenotype “fitness YPD” was calculated as 1/doubling time in YPD at 30°C. “OD saturation” refers to the OD_{595nm} at the saturation phase.

In addition, a colony-size assay was performed for high salt phenotype by replicating YPD overnight cultures on agar plates and growing them for 2-4 days, until an average colony diameter of ~5mm was reached. To determine colony sizes, photos were taken of the agar plates and processed with the CellProfiler software (CARPENTER *et al.* 2006). The relative fitness in a specific condition was calculated as: log (colony size treatment) - log (colony size control). To account for variability between plates, the colony sizes were normalized using the median colony size per plate. Colony shapes were determined by visual observation of the control plates (30°C YPD) used for the colony-size assay.

Bulk segregant analysis (BSA)

BSA was done similarly to the approach in Parts *et al.* (PARTS *et al.* 2011). In brief, two independent pools of segregants from an S96 x SK1 cross (see Yeast strain generation) were grown in 100ml YPD for 4h. From this pre-culture, 400ml of each specific condition medium (treatment) and of YPD (30°C control) were inoculated with a starting OD_{600nm} = 0.08 and grown until OD_{600nm} = 2. This dilution step was repeated to keep cells in continuous exponential growth for ~100 divisions. The cells were then collected and kept at -80°C for later DNA isolation and library preparation.

Sequencing library preparation

Genomic DNA from individual (ISA) or pooled strains (BSA) was isolated from fresh and frozen cell pellets with the PrepEase kit (USB). Adapters were ligated to sonicated DNA as previously described (WILKENING *et al.* 2013). After size selection on an E-Gel (Invitrogen), libraries were amplified with Illumina paired-end primers, cleaned, and sequenced (105 bp paired-end) on a HiSeq 2000 (Illumina).

Reciprocal Hemizygosity Scanning (RHS)

Both alleles of each gene in the genome were individually deleted in the SK1 x S96 hybrid, and replaced with a molecular barcode and a kanMX4 cassette. The resulting

RHS pools were grown for 40 generations in the following conditions: YPD 30°C, YPD 38°C, YPD + 350mM NaCl, YPD + 350µM cantharidin. Genomic DNA from the pool was extracted, the uptags and downtags containing the barcodes were amplified by PCR, and hybridized to Tag4 Microarrays (Affymetrix) (PIERCE *et al.* 2007). Fitness of each deletion strain was deduced from the signal intensity of the barcodes on the microarray. For each gene, the selection coefficient s (or relative growth rate of the strain in the pool) was estimated using the \log_2 fold change of normalized signal intensity between the initial and final timepoints (details in Supplementary Notes). The allelic effect at each locus was calculated as the difference between the selection coefficients ($\Delta s = s_{SK1} - s_{S96}$).

Confirmation of QTLs

To test the effect of a gene variant on a specific trait, the open reading frame (ORF) +/- 300bp was deleted by homologous recombination. For S96 a CORE cassette (STORICI *et al.* 2001) (kindly provided by Michael Knop) with *KIURA3* (counter-selectable) and *kanMX4* (reporter) markers was inserted by standard DNA targeting procedures (GIETZ and SCHIESTL 2007) at the respective ORF locus. For SK1 transformation was done by electroporation (as described in <http://www.koko.gov.my/CocoaBioTech/DNA%20Cells36.html>). Cells were then spread on synthetic dextrose plates supplemented with geneticin (G418, 400µg/ml) and lacking uracil for 3-4 days at 30°C. The correct integration site was confirmed by colony PCR with internal and external primers (Table S1). For allele replacement experiments, cells were transformed with the ORF region +/- 600bp amplified from the strain carrying the desired allele. Counterselection for the CORE cassette excision was performed by selection on plates containing 5-fluoroorotic acid (5-FOA, 1g/L).

Computational detection of genetic interactions

Apart from the stratification of the samples according to the major QTL, to identify QTLs acting in a specific background, the Interaction Distance method (ID) (IGNAC *et al.* 2012) was applied. ID is based on merging interaction information, a generalization of mutual information to three variables, and the normalized information distance, a metric of the amount of information shared between two variables. ID was applied to measure dependence between two genetic markers and

a phenotype, allowing us to detect the presence of interactions between the QTLs. Positive ID values indicate redundant information between markers with strong effects on the phenotype (due to linkage or genetic redundancy); negative values indicate synergy between the markers in predicting the quantitative phenotype. To estimate the statistical significance of an ID value, we computed IDs between one million randomly generated markers given the same phenotype. A candidate interaction was considered significant if its p-value was less than 0.005. In applying ID, we discretized the variables: for example, the phenotype in high temperature growth was discretized into four bins of equal size. To reduce computational requirements, we initially reduced the number of markers to 1226 by identifying blocks of highly correlated markers. Figure S2A shows the significant interaction candidates among the reduced set of markers. For the high-resolution interaction analysis in the *TAO3-MKT1* region, we then selected all markers with the appropriate coordinates from the full marker set.

Results

We performed QTL mapping on 11 distinct traits using three high-throughput approaches (BSA, ISA, and RHS). In the following, we present the QTL mapping results of these independent approaches, ranging from a simple Mendelian trait, to non-selectable traits with two to three QTLs with similar effect sizes, to complex traits driven by many QTLs with different effect sizes. Five of these traits were analyzed with all three methods, which allowed us to evaluate their performance in QTL detection. Finally, our large set of individual segregants allowed us to identify interactions between QTLs within specific phenotypes.

BSA, ISA, and RHS effectively detect the causal QTL for cantharidin resistance.

We first evaluated the three methods (ISA, BSA, and RHS) to map QTLs for a Mendelian trait (cantharidin resistance), where S96 is resistant and SK1 is sensitive to cantharidin. With ISA, we mapped a single interval of ~1kb (LOD >200) on chromosome (chr) 8 (Figure 2). Within 3kb of this interval a BSA QTL was called, with the S96 allele highly enriched (~95%); this QTL was found in both biological replicates, while several additional BSA peaks with similar amplitudes were not. The gene *CRG1* was located in the strongest QTL peak in ISA and was also the top RHS

hit (Figure 2). We confirmed the causative role of *CRG1* by individually phenotyping the RHS hemizygous strains, demonstrating that deletion of the S96 *CRG1* allele abolished cantharidin resistance (Figure S3). Individual and combinatorial replacement of the two nonsynonymous *CRG1* SNPs (D82E and Y119C) indicated that both are necessary for cantharidin resistance in S96: 60 colonies of SK1 cells carrying both SNPs grew on cantharidin plates but none from the single SNP replacements. Our results are consistent with previous reports that *CRG1* confers cantharidin resistance (NIEWMIERZYCKA and CLARKE 1999; HOON *et al.* 2008; LISSINA *et al.* 2011). *Crg1* has been shown to mediate resistance to cantharidin by direct methylation of the compound, rendering it non-toxic for yeast (LISSINA *et al.* 2011). Our results suggest that the enzymatic activity of *Crg1* or its interaction with cantharidin is impaired by this change of two amino-acids. Thus collectively, our results demonstrate that all three approaches successfully detect the true QTL for this Mendelian trait.

ISA detects QTLs for two non-selectable traits.

We next analyzed two non-selectable traits that clearly differed among the parental strains and segregants, namely colony shape and flocculation. For these traits, BSA and RHS approaches could not be performed since they use pooled phenotyping and require a selective pressure. SK1 cells form a wrinkled colony shape on agar plates, whereas S96 cells form smooth colonies (Figures S4 and S5). 8.5% of the progeny formed wrinkled colonies, which suggests that the trait is conditioned by three or four independent genes (probability of 0.5^3 to 0.5^4 when assuming the same effect size). Consistent with this estimate, we identified three QTLs which, using gene deletion and allele replacement, we narrowed down to three genes (*AMN1*, *MUC1* and *SFL1*, Figure S5) required for the wrinkled SK1-like colonies.

While neither of the parental strains flocculated, one-quarter of the segregants did (23% in rich lactose medium), suggesting that two independent genes condition the phenotype. Indeed, we detected two QTLs (Figure S4), each of which contains a gene known to modify flocculation: the *FLO1* allele (HODGSON *et al.* 1985) from the S96 background (disrupted in SK1 according to our sequencing data) and the *SFL1* allele (FUJITA *et al.* 1989) from the SK1 background (which harbors a premature stop codon at amino acid 477 in SK1). For *SFL1*, the calculated maximum LOD score in

the QTL was within the gene and even close to its premature (likely causative) stop codon in SK1. By narrowing the QTLs of these physical phenotypes down to the presumably causative genes, we demonstrate the ability of ISA to map QTLs at high resolution in these non-selective binary traits.

From simple to complex traits

In our study, the average confidence interval size for QTLs detected in ISA was 6cM (~18kb). This resolution was much higher compared to previous studies, where interval size has ranged from 16cM (STEINMETZ *et al.* 2002) to 19cM (SINHA *et al.* 2008). Given the successful identification of causative genes for less complex traits, we applied ISA to eight quantitative traits showing a continuous distribution among the segregants (Figure 3 and Table S2). We used these results to estimate the extent to which increasing the number of segregants improves the resolution of QTL detection (Figure S6 and Table S3). Our results suggest that for complex, multifactorial traits, increasing the number of segregants from 200 to at least 600 improves the resolution by more than 2-fold (Figure S6), but has no effect for Mendelian traits. Four of these complex growth traits (ethanol, 5-fluorouracil (5-FU), high salt concentration, and high temperature) were also analyzed by BSA and RHS. In contrast to the physical traits, these traits are more suitable for BSA and RHS since the fittest strains can be selected via pooled growth. However, our RHS approach displayed a high false positive rate (discussed later) and RHS results are therefore not shown.

ISA uncovers the architecture of the complex high-salt tolerance trait.

We combined ISA and BSA to dissect the high-salt tolerance trait as thoroughly as possible. At a high salt concentration (350 mM NaCl), S96 grew faster than SK1 and their progeny showed a continuous distribution of growth rates. Six QTLs were identified with ISA and eight with BSA, two of which overlapped (chr 4 and chr 16). The chr 4 QTLs were the strongest identified by each approach (Figure 4; BSA: Table S2; ISA: LOD >50, cutoff LOD = 3.5). Within the 95% confidence interval of these QTLs lies a cluster of *ENA* genes encoding sodium pumps, which are known to confer salt resistance (HARO *et al.* 1991). In contrast to a cluster of five highly similar *ENA* genes present in S96 (*ENA*1-5), SK1 carries only one copy of *ENA*6, a phylogenetically distant *ENA* gene (DARAN-LAPUJADE *et al.* 2009). *ENA* copy number

variation has been associated with high salt tolerance across different yeast strains (WARRINGER *et al.* 2011). Accordingly, we found that overexpressing *ENA6* increased salt resistance in SK1 cells (Figure S7). Moreover, we determined that *ENA* copy number accounts for 20% of the phenotypic variance. Our results thus demonstrate the ability of both ISA and BSA to successfully identify a large-effect locus.

However, identification of the major QTL is often not sufficient for understanding the genetic basis of a trait. If the sample size is too small, the phenotypic variance caused by a large effect QTL like the *ENA* locus can be overestimated and the QTLs with smaller effects will be obscured. To overcome this risk and identify additional QTLs for salt tolerance, we stratified the ISA segregants according to their *ENA* genotype and repeated the QTL analysis. This highlighted the contribution of QTLs with high LOD scores (chr 3, 5, 14, 15, 16) even in the detrimental SK1 *ENA* background (Figure 4). We thus identified six QTLs that explain more than 80% of both narrow (additive genetic factors) and broad sense heritability (all genetic factors including genetic interactions) (VISSCHER *et al.* 2008) (Table S4), suggesting that we have captured most of the causative alleles. These results demonstrate that allelic stratification can reveal additional QTLs and thus enable a more comprehensive dissection of complex traits.

Six of eight BSA QTLs were specific to BSA, in which cells were cultured for 5-9 days (versus 1-2 days in ISA). To test whether the difference in QTL detection could be attributed to long-term effects, we performed a colony size assay on agar with the ISA segregants (2-4 days in culture). In segregants with the S96 *ENA* background, we observed a beneficial effect on chr 9, where one of the BSA-specific QTLs was also detected (Figure 4). This observation suggests that variations in experimental procedures, such as assay duration, can lead to the detection of different QTLs. The combination of several methods could thus be a strategy to more thoroughly resolve the alleles responsible for a complex trait.

Mapping of high temperature QTLs reveals major differences between ISA and BSA.

We then applied both BSA and ISA to dissect another selective phenotype, high temperature growth. At high temperature (38°C), S96 grew faster than SK1 and five

QTLs were identified with ISA and three with BSA. Only the QTL on chr 9 (S96 allele beneficial) was common between these two approaches (Figure 5). Within this QTL, we identified *TAO3* as the gene responsible for high temperature resistance, which we confirmed by allele replacement. By applying the stratification method described in the previous section, we identified additional smaller effect QTLs that act specifically in the SK1-*TAO3* or the S96-*TAO3* background. We were able to separate a double LOD peak on chr 14 (Figure 5, lower right image): the left peak was mapped in the SK1 *TAO3* background, and the right peak (including *MKT1*) in the S96 *TAO3* background. By generating strains with all four combinations of *TAO3* and *MKT1* alleles in the S96 background, we confirmed that the effect of the *MKT1* variant was indeed larger in combination with the S96 *TAO3* allele (Figure 5, lower left image). These results show that the resolution of our ISA approach is sufficient to identify two QTLs within a distance of less than 100kb (Figure 5), and demonstrate the power of ISA for detecting epistatic genetic interactions. The identified QTLs explain ~59% and 47% of the narrow sense and broad sense heritability respectively (Table S4), suggesting that several additional causative alleles remain undiscovered.

Mapping genetic loci associated with growth on ethanol, glycerol, and 5-FU.

For growth with ethanol as the carbon source (YPE), both ISA and BSA detected a QTL on chr 14 and the SK1 allele of *MKT1* was confirmed as causative for improving growth in YPE by allele replacement (Figure S7 and S8). In addition to its impact on high temperature growth, we also confirmed that the SK1 allele of *TAO3* (lying within a major ISA QTL on chr 9) significantly improves growth in media containing glycerol as the carbon source (YPG) (Figure S7). Finally, for growth in 5-Fluorouracil (5-FU), one QTL was identified by both ISA and BSA on chr 5 (likely due to a *URA3* deletion in the SK1 background). None of the other BSA QTLs were reproducible between the two biological replicates (Figure S8). Using ISA, however, we successfully identified and confirmed by allele replacement that *MKT1* (within the QTL of chr 14) is causative for improved growth on 5-FU.

ISA allows the detection and characterization of genetic interactions.

The complete dissection of complex traits can be hindered by non-additive genetic interactions, but also by the presence of closely linked alleles, which often remain undetected despite their contribution to phenotype. We previously reported one such

linked region surrounding *MKT1* on chr 14 (STEINMETZ *et al.* 2002), which could explain the missing heritability (both narrow and broad) observed for high-temperature growth. In fact, the experimentally validated *MKT1-TAO3* interaction responsible for high-temperature growth lies in regions of high linkage. We observed that the LOD profile for high-temperature growth has many local peaks on chr 9 and chr 14, which carry *TAO3* and *MKT1* respectively (Figure S2A). If we include all markers on chr 9 and chr 14 for estimating the heritability, more than 65% of both narrow and broad sense heritability can be explained (Table S4), suggesting the presence of closely linked, interacting QTLs. To dissect these interactions at a finer resolution, we applied an interaction distance method (IGNAC *et al.* 2012). A subset of 1226 markers was used to identify regions with the strongest interactions on chr 9 and chr 14. These regions of interaction were further analyzed with a denser marker set, and our results suggest that both regions contain more than one causative locus, and that these loci interact with each other (Figure S2A).

The interaction Distance method (IGNAC *et al.* 2012) allowed us to detect both redundancy and synergistic effects between ISA QTLs for growth in YPE and YPD (Table S5 and Figure S2B). Our results demonstrate that ISA is a powerful method to detect and characterize genetic interactions, which must be accounted for to explain phenotypic variance in complex traits.

Several factors confound QTL detection in pooled approaches.

We next assessed the impact of experimental factors that confound QTL identification for each approach, which may partly explain their differing results. While for most traits, BSA QTLs of both biological replicates were nearly identical, they varied widely between replicates for resistance to cantharidin and 5-FU (Figure 2 and Figure S8). Sequencing the 5-FU BSA pools revealed nonsense mutations in genes conferring resistance to the drug (*FUR4*, *URA2*), suggesting that individual cells acquired beneficial mutations and overtook the population, causing the enrichment of false positive loci. This effect is specific to bulk selection approaches, and is likely to occur for all phenotypes for which single mutations can confer a significant growth advantage. The impact of such confounding mutations would be expected to increase with the strength and length of the selection procedure.

Besides mutations that cause resistance in BSA and aneuploidy in RHS, we determined diploidization to be another confounding factor during long-term selection in BSA. We sequenced BSA pools at different timepoints during selection at high temperature. A decrease of an initially strong SK1 allele enrichment on chr 3 (from ~100% to 50% allele frequency) was observed between generations 16 and 24 (Figure S10). This loss was detected in all of our BSA experiments and can also be observed in other studies (EHRENREICH *et al.* 2010). This enrichment of SK1 alleles on chr 3 corresponds to the *MATa* locus used for the initial selection of haploid progeny for BSA. Mating-type PCR (HUXLEY *et al.* 1990) performed on 32 individual clones after 100 generations confirmed that all cells had become diploid at this stage. This implies that a small number of *MATalpha* cells in the initial BSA pool mated with *MATa* cells, and that these diploid cells then overtook the population.

As described earlier, RHS results displayed a high rate of false positive hits for our complex traits. Resequencing 50 of the RHS deletion strains revealed numerous chromosomal aberrations, which mostly consisted of triploidies. 12 of 38 false positive strains and four of 12 randomly selected strains were aneuploid (see Table S6 and Figure S9 for details). Since these aberrations affect many genes, their consequences are likely to obscure allelic differences at a single locus, especially when these are more subtle as for complex traits, and can thus lead to false positives.

These observations suggest that both pooled methods are vulnerable to genetic alterations that can render the detection of truly causative QTLs difficult. These confounding factors should therefore be taken into account by adapting the experimental approaches, for example by decreasing the duration of selective pressure, or comparing additional biological replicates.

Discussion

Despite intensive efforts, dissecting the genetic basis of complex traits is a persistent challenge. Several methods have been developed, including pooled approaches such as BSA, allowing for millions of individuals to be tested in a single experiment.

Using next-generation sequencing techniques, a large numbers of segregants can now be individually genotyped at a reasonable cost (WILKENING *et al.* 2013), enabling higher-resolution QTL mapping. To further increase resolution to the level of individual genes, we also developed and applied the RHS method. In the following section, we discuss the biological impact of quantitative trait gene (QTG) identification for two dissected traits (wrinkled colony shape and flocculation), confounding factors of pooled approaches like BSA and RHS, and the importance of interactions between QTLs.

QTGs for wrinkled colony shape and flocculation are closely related.

For wrinkled colony shape we identified three QTGs (Figure S4), which are also known to modify flocculation. Among these, *AMN1* encodes a protein required for daughter cell separation (WANG *et al.* 2003) and cell clumpiness (YVERT *et al.* 2003). It has not been associated with colony shape before, but was recently implicated in flocculation (LI *et al.* 2013). Moreover, a loss-of-function mutation in the S96 *AMN1* allele (D368V) has been reported to cause widespread gene expression changes (YVERT *et al.* 2003; RONALD *et al.* 2005). Another gene we identified as linked to flocculation is *MUC1* (also known as *FLO11*), which encodes a key cell surface protein required for flocculation, as well as invasive and pseudohyphal growth (LO and DRANGINIS 1998). Furthermore, the number of serine/threonine-rich tandem repeats in *MUC1* has been linked to flocculation strength (VERSTREPEN *et al.* 2005; LIU *et al.* 2007), and this region is 1.1kb shorter in SK1, corresponding to ~12 repeats vs. 40 repeats in S96 (for primer sequences see Table S1). *MUC1* expression level has also been connected to colony shape (BARRALES *et al.* 2008; WHITE *et al.* 2011; VOORDECKERS *et al.* 2012). The third gene we identified is *SFL1*, which is a known flocculation inhibitor (FUJITA *et al.* 1989). Its deletion causes wrinkled colony shape in the Σ1278b background (HALME *et al.* 2004), which is consistent with our observation that the SK1 allele of *SFL1* with its premature stop codon is required for wrinkled colony shape. Despite *AMN1*, *MUC1*, and *FLO5* having previously been implicated in flocculation (GOVENDER *et al.* 2008; LI *et al.* 2013) and the first two genes showing an effect on colony morphology in our study, we did not see any effect of these polymorphisms on flocculation in our background, as no QTLs for flocculation were detected at these genes. However, *SFL1* was detected as a QTL for both traits.

Two pleiotropic genes were identified across the traits tested.

We confirmed by allele replacement that two QTGs modify multiple phenotypes (*TAO3*, *MKT1*) (Figure 3). We found that the SK1 allele of the well-known pleiotropic gene *MKT1* was beneficial for three growth phenotypes (high temperature, YPE, and 5-FU, Figure 3 and Figure S7). Previous studies have found *MKT1* to modify high temperature (STEINMETZ *et al.* 2002), sporulation (DEUTSCHBAUER and DAVIS 2005), petite frequency (DIMITROV *et al.* 2009), DNA repair (DEMOGINES *et al.* 2008a) or drug sensitivity (KIM and FAY 2009; EHRENREICH *et al.* 2010). The most likely causative polymorphism is a D30G mutation, with G being conserved across all other sequenced strains (SWINNEN *et al.* 2011). Moreover, as reported by Zhu *et al.* (ZHU *et al.* 2008), *MKT1* is a global regulator of gene expression and can therefore influence many traits. Similarly, *TAO3* was identified as a QTG in two phenotypes (high temperature and YPG, Figure 3 and Figure S7) in our study. This gene has previously been identified as a causative QTG for sporulation (DEUTSCHBAUER and DAVIS 2005) in the same strain background (SK1 x S96), but has not been connected to high temperature resistance before our study. Finally, the implication of *SFL1* in colony shape in this study along with its previous implication in flocculation (FUJITA *et al.* 1989) suggests that this gene is also pleiotropic. On the other hand, QTLs identified for growth in three different non-fermentable carbon sources (lactose = YPL, ethanol = YPE, glycerol = YPG) did not overlap (Figure 3), suggesting the absence of gene variants that globally influence the metabolism of non-fermentable carbon sources (e.g. enzymes of the Krebs cycle or mitochondrial respiration) in our strain background.

Analyses of pooled approaches suggests potential confounding factors.

Unlike morphological traits, phenotypes that confer a growth advantage under a specific condition are especially suited for BSA and RHS, as phenotypic selection can be performed in bulk. The BSA approach is relatively fast and easy and confers a significant advantage over the other two approaches in terms of time and cost. However, we observed that spontaneous mutations conferring resistance to the selective pressure can lead to biased results. Assuming a low number of cells with an advantageous mutation in the original BSA pool, a shorter selection time (e.g. 10-30 generations) might alleviate this effect. Moreover, the analysis of multiple

timepoints and biological replicates should help to identify true QTLs for traits with a strong selective pressure.

Additionally, the use of a BSA pool with haploid segregants harbors the risk of diploidization, as seen in our time-dependent high-temperature QTL maps (Figure S10). This observation is in accordance with a recent study showing the invasion of diploids in a population of haploids despite no apparent growth advantage (GERSTEIN and OTTO 2011). The presence of heterozygous strains diminishes the enrichment of beneficial alleles, since for dominant alleles the allele frequency would rarely reach 100% because of recessive allele remaining in the heterozygous strains. To avoid the diploidization of haploid segregants in BSA, the strains could be diploidized in advance. The haploid segregants could also be independently phenotyped, followed by genotyping the pool of strains with extreme phenotypes. Nevertheless, even this method would still be limited by large-effect QTLs masking smaller-effect QTLs. Moreover, as explained earlier, genetic interactions are not detectable with BSA, nor does it allow the separation of linked QTLs. Thus, combining the modified BSA strategies above with ISA should compensate for these limitations and lead to a more comprehensive understanding of the genetic architecture of complex traits.

The genome-wide RHS approach developed in our laboratory is based on individual gene deletions and successfully identified the causative gene for a Mendelian trait (cantharidin resistance). It should theoretically have performed best at identifying individual causative genes; nevertheless, it displayed a high false positive rate for complex traits, most likely caused by chromosomal aberrations (Figure S9). A related recent study also reported incidences of aneuploidies and mutations, leading to high false positive rates (KIM *et al.* 2012). This issue could be circumvented either by sequencing all strains and eliminating aberrant genotypes, or by constructing additional replicate strains. With the emergence of more efficient gene editing techniques, e.g., CRISPR/Cas (CONG *et al.* 2013), an RHS-type approach could also be feasible in the near future for human cells, which should enhance the detection of functional alleles for phenotypes with medical implications (e.g. drug resistance, cancer development and progression).

Different culture times might contribute to BSA-ISA differences.

For high salt resistance, different QTLs were detected between BSA and ISA. One factor likely contributing to these differences is the longer culture time in BSA. Our results using a longer-term colony assay in ISA (Figure 4) suggest that in the BSA pool, an early selection for the advantageous S96 *ENA* allele occurred, followed by enrichment of beneficial alleles in this background. This effect has also been observed in two studies, which identified different QTLs depending on sporulation time (DEUTSCHBAUER and DAVIS 2005; BEN-ARI *et al.* 2006). This selection for large-effect QTLs and the subsequent enrichment of additional alleles in this background is a caveat to BSA studies, as QTLs acting specifically in the presence of the detrimental major QTL allele would be overlooked. This problem can be avoided by using ISA, where genotypic stratification of segregants can be performed.

Gene-gene interactions and linked QTLs hinder the identification of QTGs.

Besides large-effect QTLs masking the genetic effects of other causative genes, the difficulty of dissecting quantitative traits is increased by two factors even in an ISA approach. First, synergistic interactions can occur between functionally related genes (PEREZ-PEREZ *et al.* 2009). With the interaction distance method we detected synergistic gene-gene interactions, similarly to Bloom *et al.* (BLOOM *et al.* 2013), as well as redundancy effects (Table S5). We found very little overlap between these interaction pairs and those found using synthetic lethality screens (TONG *et al.* 2001; TONG *et al.* 2004), suggesting that natural and synthetic variant interactions may shape phenotypic robustness differently. Second, a group of tightly linked genes can be responsible for large-effect QTLs (NOOR *et al.* 2001). With the high-temperature growth phenotype, we confirmed the novel *TAO3-MKT1* interaction, and many more are expected from our Interaction Distance Method (Figure S2). These results suggest that effects of linked causative genes and synergy are prevalent, and should be accounted for in future efforts to map quantitative traits. Parts *et al.* have shown that multiple rounds of crossing from generations F1 to F12 can reduce the linkage between two loci (PARTS *et al.* 2011), an approach that could thus increase QTL resolution and dissect linked QTGs.

In conclusion, our study addresses the fundamental issue of how to improve quantitative trait dissection. Applying three high-throughput approaches allowed us to resolve eight potential causative genes for eight phenotypes. Nevertheless, for the

complex traits, the causal alleles explained only part of the heritability (on average ~60% of broad sense and ~66% of narrow sense; Table S4), suggesting the contribution of additional factors such as linked QTLs and epistatic effects. To thoroughly assess the impact of these factors on phenotype, future studies should improve resolution by increasing the sample size. Future studies would also benefit from accounting for experimental differences that can influence the loci detected, for example by combining multiple approaches as we have done here. Our findings indicate that we are currently looking at the tip of the iceberg: the focus should now be placed on the development of innovative experimental and computational strategies to deepen our understanding of the complex architecture of quantitative traits.

Acknowledgements

We thank Vicent Pelechano for fruitful discussions, and Michael Knop for providing materials. We also thank Wu Wei and Leopold Parts for valuable feedback on the manuscript. This study was technically supported by the EMBL Genomics Core Facility, where the libraries were sequenced. Our research received funding from the Deutsche Forschungsgemeinschaft (DFG-GZ: WI 3311/2-1) to S.W. and from the National Institutes of Health, the Deutsche Forschungsgemeinschaft (1422/2-2), and the European Research Council under the European Union's Seventh Framework Programme (FP7/2007-2013) / ERC Grant agreement n° AdG-294542 to L.M.S.

Author Contributions

L.M.S., S.W., A.D., and E.S.F conceived and designed the experiments. S.W., G.L., E.S.F., M.M.T., R.K., and M.R. performed the experiments. G.L., S.A., N.S., D.G., and J.G. analyzed the data. G.L., S.A., N.A.S., D.G., J.G., and M.P. contributed reagents/materials/analysis tools. S.W., G.L., E.S.F., R.S.A and L.M.S. wrote the paper.

Disclosure declaration

The authors declare that they have no competing financial interests.

Supplementary information

Supplementary notes, tables and figures can be found in the online version of the paper.

Figure legends

Figure 1. Schematic overview of the three QTL mapping approaches used in this study. The parental strain backgrounds S96 and SK1 were used for all approaches. Individual segregant analysis (ISA): genotyping and phenotyping are performed on individual segregants. Bulk segregant analysis (BSA): a pool of segregants is grown in control and selective media. By sequencing the pooled genomic DNA, the allelic enrichments in the pool are determined. Reciprocal hemizygosity scanning (RHS): in a hybrid strain, alleles are alternatively deleted, resulting in reciprocal hemizygous, isogenic hybrid strains that differ only by a single allele. DNA barcodes specific to each gene enable the pooling and parallel analysis of strain fitness on a genome-wide level. After selective growth, the barcodes are amplified and hybridized to a microarray, providing a proxy of fitness that can be used to measure the effects of allelic variation in each gene on the phenotype of interest.

Figure 2. Cantharidin resistance QTLs mapped by BSA, ISA, and RHS. The top LOD (logarithm of odds) score identified by ISA is located directly at the causal *CRG1* gene, which was also the top hit in RHS (bottom plot). For BSA, the SK1 allele frequency (1 corresponding to 100% SK1, 0 to 100% S96) is plotted for two biological replicates. These replicates were not reproducible overall (likely due to spontaneous beneficial mutations in individual cells of the pool, as seen for 5-FU treatment), except for very few regions (including the *CRG1* locus). The results on chr 8, which contains *CRG1*, are magnified (inset). For RHS, Δs represents the difference between the selection coefficients of S96 and SK1.

Figure 3. Detection of ISA QTLs for 11 phenotypes. LOD scores are plotted for all phenotypes tested in this study using the IGV browser (Robinson et al. 2011) (Mendelian traits = blue, fitness traits in rich media = black, high temperature = red, high salt (NaCl) = green, non-fermentable carbon sources = purple, 5-FU = gray). QTLs containing putative causative variants are marked with a gray dashed line and

labeled with the gene. Gene variants that were confirmed by allele exchange or by individual growth of RHS strains (for *CRG1*) in this study are marked with a star at the respective phenotype. Two gene variants were found to modify more than one phenotype: *MKT1* (high temperature, ethanol, 5-FU) and *TAO3* (high temperature, glycerol).

Figure 4. Identification of high salt QTLs. For BSA, SK1 allele frequency is plotted in black (replicates were highly reproducible and therefore only one is shown). For ISA results, the LOD scores are plotted in green. In addition to the standard method (1-2 days liquid culture), ISA phenotyping was also performed by a colony size assay on agar (2-4 days), in order to account for effects of growth duration. The major QTL identified by all approaches was the *ENA* locus on chr 4 (*ENA* CNV), which contains a cluster of genes encoding sodium pumps. By stratifying the ISA samples according to their *ENA* genotype (S96 *ENA* = red, SK1 *ENA* = blue), QTLs specific to SK1 *ENA* (chr 3 and chr 15 for liquid culture) and S96 *ENA* (chr 9 for colony size assay) were detected. The synergistic effect of the QTL on chr 9 in combination with *ENA* is also illustrated in the boxplot using the individual fitness (according to colony size) of 720 segregants. To test for interactions, we used an ANOVA test. A linear model is fitted to the data: phenotype ~ QTL1 + QTL2 + QTL1:QTL2. The p-value for the interaction is the significance of including the interaction term (QTL1:QTL2).

Figure 5. Identification of high temperature QTLs. BSA and ISA results are plotted as in Figure 4. By stratifying the ISA samples for the major QTL (S96 *TAO3* = red, SK1 *TAO3* = blue), the double QTL peak on chr 14 could be separated into two individual QTLs; chr14:390,000-410,000 for the SK1 *TAO3* subset and chr14:480,000-500,000 for the S96 *TAO3* subset. A magnification of this region is shown in the bottom right panel, with 95% confidence intervals and the calculated maximum shown as boxes below the separated peaks. The synergistic interaction between the S96 *TAO3* and the SK1 *MKT1* was confirmed in 94 allele replacement strains (bottom left boxplot). The p-value for interaction was calculated as described in the legend of Figure 4.

Literature Cited

Barrales, R. R., J. Jimenez and J. I. Ibeas, 2008 Identification of novel activation mechanisms for FLO11 regulation in *Saccharomyces cerevisiae*. *Genetics* 178: 145-156.

Ben-Ari, G., D. Zenvirth, A. Sherman, L. David, M. Klutstein *et al.*, 2006 Four linked genes participate in controlling sporulation efficiency in budding yeast. *PLoS Genet* 2: e195.

Birkeland, S. R., N. Jin, A. C. Ozdemir, R. H. Lyons, Jr., L. S. Weisman *et al.*, 2010 Discovery of mutations in *Saccharomyces cerevisiae* by pooled linkage analysis and whole-genome sequencing. *Genetics* 186: 1127-1137.

Bloom, J. S., I. M. Ehrenreich, W. T. Loo, T. L. Lite and L. Kruglyak, 2013 Finding the sources of missing heritability in a yeast cross. *Nature* 494: 234-237.

Brem, R. B., J. D. Storey, J. Whittle and L. Kruglyak, 2005 Genetic interactions between polymorphisms that affect gene expression in yeast. *Nature* 436: 701-703.

Broman, K. W., H. Wu, S. Sen and G. A. Churchill, 2003 R/qtl: QTL mapping in experimental crosses. *Bioinformatics* 19: 889-890.

Browning, S. R., and B. L. Browning, 2007 Rapid and accurate haplotype phasing and missing-data inference for whole-genome association studies by use of localized haplotype clustering. *American journal of human genetics* 81: 1084-1097.

Carpenter, A. E., T. R. Jones, M. R. Lamprecht, C. Clarke, I. H. Kang *et al.*, 2006 CellProfiler: image analysis software for identifying and quantifying cell phenotypes. *Genome Biol* 7: R100.

Cong, L., F. A. Ran, D. Cox, S. Lin, R. Barretto *et al.*, 2013 Multiplex genome engineering using CRISPR/Cas systems. *Science* 339: 819-823.

Daran-Lapujade, P., J. M. Daran, M. A. Luttik, M. J. Almering, J. T. Pronk *et al.*, 2009 An atypical PMR2 locus is responsible for hypersensitivity to sodium and lithium cations in the laboratory strain *Saccharomyces cerevisiae* CEN.PK113-7D. *FEMS Yeast Res* 9: 789-792.

Demogines, A., E. Smith, L. Kruglyak and E. Alani, 2008a Identification and dissection of a complex DNA repair sensitivity phenotype in Baker's yeast. *PLoS Genet* 4: e1000123.

Demogines, A., A. Wong, C. Aquadro and E. Alani, 2008b Incompatibilities involving yeast mismatch repair genes: a role for genetic modifiers and implications for disease penetrance and variation in genomic mutation rates. *PLoS genetics* 4: e1000103.

Deutschbauer, A. M., and R. W. Davis, 2005 Quantitative trait loci mapped to single-nucleotide resolution in yeast. *Nat Genet* 37: 1333-1340.

Dimitrov, L. N., R. B. Brem, L. Kruglyak and D. E. Gottschling, 2009 Polymorphisms in multiple genes contribute to the spontaneous mitochondrial genome instability of *Saccharomyces cerevisiae* S288C strains. *Genetics* 183: 365-383.

Ehrenreich, I. M., J. P. Gerke and L. Kruglyak, 2009 Genetic dissection of complex traits in yeast: insights from studies of gene expression and other phenotypes in the BYxRM cross. *Cold Spring Harbor symposia on quantitative biology* 74: 145-153.

Ehrenreich, I. M., N. Torabi, Y. Jia, J. Kent, S. Martis *et al.*, 2010 Dissection of genetically complex traits with extremely large pools of yeast segregants. *Nature* 464: 1039-1042.

Endelman, J. B., 2011 Ridge Regression and Other Kernels for Genomic Selection with R Package rrBLUP. *Plant Gen.* 4: 250-255.

Flint, J., 2011 Mapping quantitative traits and strategies to find quantitative trait genes. *Methods* 53: 163-174.

Flint, J., and T. F. Mackay, 2009 Genetic architecture of quantitative traits in mice, flies, and humans. *Genome Res* 19: 723-733.

Foss, E. J., D. Radulovic, S. A. Shaffer, D. M. Ruderfer, A. Bedalov *et al.*, 2007 Genetic basis of proteome variation in yeast. *Nature genetics* 39: 1369-1375.

Fujita, A., Y. Kikuchi, S. Kuhara, Y. Misumi, S. Matsumoto *et al.*, 1989 Domains of the SFL1 protein of yeasts are homologous to Myc oncoproteins or yeast heat-shock transcription factor. *Gene* 85: 321-328.

Gatbonton, T., M. Imbesi, M. Nelson, J. M. Akey, D. M. Ruderfer *et al.*, 2006 Telomere length as a quantitative trait: genome-wide survey and genetic mapping of telomere length-control genes in yeast. *PLoS Genet* 2: e35.

Gerstein, A. C., and S. P. Otto, 2011 Cryptic fitness advantage: diploids invade haploid populations despite lacking any apparent advantage as measured by standard fitness assays. *PLoS One* 6: e26599.

Gietz, R. D., and R. H. Schiestl, 2007 High-efficiency yeast transformation using the LiAc/SS carrier DNA/PEG method. *Nat Protoc* 2: 31-34.

Govender, P., J. L. Domingo, M. C. Bester, I. S. Pretorius and F. F. Bauer, 2008 Controlled expression of the dominant flocculation genes FLO1, FLO5, and FLO11 in *Saccharomyces cerevisiae*. *Appl Environ Microbiol* 74: 6041-6052.

Halme, A., S. Bumgarner, C. Styles and G. R. Fink, 2004 Genetic and epigenetic regulation of the FLO gene family generates cell-surface variation in yeast. *Cell* 116: 405-415.

Haro, R., B. Garciaideblas and A. Rodriguez-Navarro, 1991 A novel P-type ATPase from yeast involved in sodium transport. *FEBS Lett* 291: 189-191.

Heck, J. A., J. L. Argueso, Z. Gemici, R. G. Reeves, A. Bernard *et al.*, 2006 Negative epistasis between natural variants of the *Saccharomyces cerevisiae* MLH1 and PMS1 genes results in a defect in mismatch repair. *Proceedings of the National Academy of Sciences of the United States of America* 103: 3256-3261.

Hodgson, J. A., D. R. Berry and J. R. Johnston, 1985 Discrimination by heat and proteinase treatments between flocculent phenotypes conferred on *Saccharomyces cerevisiae* by the genes FLO1 and FLO5. *J Gen Microbiol* 131: 3219-3227.

Hoon, S., A. M. Smith, I. M. Wallace, S. Suresh, M. Miranda *et al.*, 2008 An integrated platform of genomic assays reveals small-molecule bioactivities. *Nat Chem Biol* 4: 498-506.

Hu, X. H., M. H. Wang, T. Tan, J. R. Li, H. Yang *et al.*, 2007 Genetic dissection of ethanol tolerance in the budding yeast *Saccharomyces cerevisiae*. *Genetics* 175: 1479-1487.

Huxley, C., E. D. Green and I. Dunham, 1990 Rapid assessment of *S. cerevisiae* mating type by PCR. *Trends Genet* 6: 236.

Ignac, T. M., N. A. Sakhanenko, A. Skupin and D. J. Galas, 2012 New methods for finding associations in large data sets: Generalizing the maximal information coefficient (MIC). *Proceedings of the Ninth International Workshop on Computational Systems Biology (2012)*.

Kim, H. S., and J. C. Fay, 2009 A combined-cross analysis reveals genes with drug-specific and background-dependent effects on drug sensitivity in *Saccharomyces cerevisiae*. *Genetics* 183: 1141-1151.

Kim, H. S., J. Huh, L. Riles, A. Reyes and J. C. Fay, 2012 A noncomplementation screen for quantitative trait alleles in *Saccharomyces cerevisiae*. *G3 (Bethesda)* 2: 753-760.

Lango Allen, H., K. Estrada, G. Lettre, S. I. Berndt, M. N. Weedon *et al.*, 2010 Hundreds of variants clustered in genomic loci and biological pathways affect human height. *Nature* 467: 832-838.

Li, J., L. Wang, X. Wu, O. Fang, L. Wang *et al.*, 2013 Polygenic molecular architecture underlying non-sexual cell aggregation in budding yeast. *DNA Res* 20: 55-66.

Lissina, E., B. Young, M. L. Urbanus, X. L. Guan, J. Lowenson *et al.*, 2011 A Systems Biology Approach Reveals the Role of a Novel Methyltransferase in Response to Chemical Stress and Lipid Homeostasis. *PLoS Genet* 7: e1002332.

Liti, G., D. M. Carter, A. M. Moses, J. Warringer, L. Parts *et al.*, 2009 Population genomics of domestic and wild yeasts. *Nature* 458: 337-341.

Liu, N., D. Wang, Z. Y. Wang, X. P. He and B. Zhang, 2007 Genetic basis of flocculation phenotype conversion in *Saccharomyces cerevisiae*. *FEMS Yeast Res* 7: 1362-1370.

Lo, W. S., and A. M. Dranginis, 1998 The cell surface flocculin Flo11 is required for pseudohyphae formation and invasion by *Saccharomyces cerevisiae*. *Mol Biol Cell* 9: 161-171.

Marullo, P., M. Aigle, M. Bely, I. Masneuf-Pomarede, P. Durrens *et al.*, 2007 Single QTL mapping and nucleotide-level resolution of a physiologic trait in wine *Saccharomyces cerevisiae* strains. *FEMS yeast research* 7: 941-952.

McKenna, A., M. Hanna, E. Banks, A. Sivachenko, K. Cibulskis *et al.*, 2010 The Genome Analysis Toolkit: a MapReduce framework for analyzing next-generation DNA sequencing data. *Genome research* 20: 1297-1303.

Mumberg, D., R. Muller and M. Funk, 1995 Yeast vectors for the controlled expression of heterologous proteins in different genetic backgrounds. *Gene* 156: 119-122.

Niewmierzycka, A., and S. Clarke, 1999 S-Adenosylmethionine-dependent methylation in *Saccharomyces cerevisiae*. Identification of a novel protein arginine methyltransferase. *J Biol Chem* 274: 814-824.

Nogami, S., Y. Ohya and G. Yvert, 2007 Genetic complexity and quantitative trait loci mapping of yeast morphological traits. *PLoS Genet* 3: e31.

Noor, M. A., A. L. Cunningham and J. C. Larkin, 2001 Consequences of recombination rate variation on quantitative trait locus mapping studies. Simulations based on the *Drosophila melanogaster* genome. *Genetics* 159: 581-588.

Pan, X., D. S. Yuan, D. Xiang, X. Wang, S. Sookhai-Mahadeo *et al.*, 2004 A robust toolkit for functional profiling of the yeast genome. *Mol Cell* 16: 487-496.

Parts, L., F. A. Cubillos, J. Warringer, K. Jain, F. Salinas *et al.*, 2011 Revealing the genetic structure of a trait by sequencing a population under selection. *Genome research* 21: 1131-1138.

Perez-Perez, J. M., H. Candela and J. L. Micol, 2009 Understanding synergy in genetic interactions. *Trends Genet* 25: 368-376.

Perlstein, E. O., D. M. Ruderfer, D. C. Roberts, S. L. Schreiber and L. Kruglyak, 2007 Genetic basis of individual differences in the response to small-molecule drugs in yeast. *Nature genetics* 39: 496-502.

Pierce, S. E., R. W. Davis, C. Nislow and G. Giaever, 2007 Genome-wide analysis of barcoded *Saccharomyces cerevisiae* gene-deletion mutants in pooled cultures. *Nat Protoc* 2: 2958-2974.

Proctor, M., M. L. Urbanus, E. L. Fung, D. F. Jaramillo, R. W. Davis *et al.*, 2011 The automated cell: compound and environment screening system (ACCESS) for chemogenomic screening. *Methods Mol Biol* 759: 239-269.

Ronald, J., R. B. Brem, J. Whittle and L. Kruglyak, 2005 Local regulatory variation in *Saccharomyces cerevisiae*. *PLoS Genet* 1: e25.

Schacherer, J., J. A. Shapiro, D. M. Ruderfer and L. Kruglyak, 2009 Comprehensive polymorphism survey elucidates population structure of *Saccharomyces cerevisiae*. *Nature* 458: 342-345.

Segre, A. V., A. W. Murray and J. Y. Leu, 2006 High-resolution mutation mapping reveals parallel experimental evolution in yeast. *PLoS Biol* 4: e256.

Sinha, H., L. David, R. C. Pascon, S. Clauer-Münster, S. Krishnakumar *et al.*, 2008 Sequential Elimination of Major-Effect Contributors Identifies Additional Quantitative Trait Loci Conditioning High-Temperature Growth in Yeast. *Genetics* 180: 1661-1670.

St Onge, R. P., R. Mani, J. Oh, M. Proctor, E. Fung *et al.*, 2007 Systematic pathway analysis using high-resolution fitness profiling of combinatorial gene deletions. *Nat Genet* 39: 199-206.

Steinmetz, L. M., and R. W. Davis, 2004 Maximizing the potential of functional genomics. *Nat Rev Genet* 5: 190-201.

Steinmetz, L. M., H. Sinha, D. R. Richards, J. I. Spiegelman, P. J. Oefner *et al.*, 2002 Dissecting the architecture of a quantitative trait locus in yeast. *Nature* 416: 326-330.

Storici, F., L. K. Lewis and M. A. Resnick, 2001 In vivo site-directed mutagenesis using oligonucleotides. *Nat Biotechnol* 19: 773-776.

Stranger, B. E., E. A. Stahl and T. Raj, 2011 Progress and promise of genome-wide association studies for human complex trait genetics. *Genetics* 187: 367-383.

Swinnen, S., K. Schaerlaekens, T. Pais, J. Claesen, G. Hubmann *et al.*, 2012 Identification of novel causative genes determining the complex trait of high ethanol tolerance in yeast using pooled-segregant whole-genome sequence analysis. *Genome Res* 22: 975-984.

Swinnen, S., J. M. Thevelein and E. Nevoigt, 2011 Genetic mapping of quantitative phenotypic traits in *Saccharomyces cerevisiae*. *FEMS yeast research*.

Tong, A. H., M. Evangelista, A. B. Parsons, H. Xu, G. D. Bader *et al.*, 2001 Systematic genetic analysis with ordered arrays of yeast deletion mutants. *Science* 294: 2364-2368.

Tong, A. H., G. Lesage, G. D. Bader, H. Ding, H. Xu *et al.*, 2004 Global mapping of the yeast genetic interaction network. *Science* 303: 808-813.

Verstrepen, K. J., A. Jansen, F. Lewitter and G. R. Fink, 2005 Intronogenic tandem repeats generate functional variability. *Nat Genet* 37: 986-990.

Visscher, P. M., W. G. Hill and N. R. Wray, 2008 Heritability in the genomics era--concepts and misconceptions. *Nat Rev Genet* 9: 255-266.

Voordeckers, K., D. De Maeyer, E. van der Zande, M. D. Vinces, W. Meert *et al.*, 2012 Identification of a complex genetic network underlying *Saccharomyces cerevisiae* colony morphology. *Mol Microbiol* 86: 225-239.

Wang, Y., T. Shirogane, D. Liu, J. W. Harper and S. J. Elledge, 2003 Exit from exit: resetting the cell cycle through Amn1 inhibition of G protein signaling. *Cell* 112: 697-709.

Warringer, J., E. Zorgo, F. A. Cubillos, A. Zia, A. Gjuvsland *et al.*, 2011 Trait variation in yeast is defined by population history. *PLoS Genet* 7: e1002111.

Wenger, J. W., K. Schwartz and G. Sherlock, 2010 Bulk segregant analysis by high-throughput sequencing reveals a novel xylose utilization gene from *Saccharomyces cerevisiae*. *PLoS Genet* 6: e1000942.

White, M. G., S. Piccirillo, V. Dusevich, D. J. Law, T. Kapros *et al.*, 2011 Flo11p adhesin required for meiotic differentiation in *Saccharomyces cerevisiae* minicolonies grown on plastic surfaces. *FEMS Yeast Res* 11: 223-232.

Wilkening, S., M. M. Tekkedil, G. Lin, E. S. Fritsch, W. Wei *et al.*, 2013 Genotyping 1000 yeast strains by next-generation sequencing. *BMC Genomics* 14: 90.

Winzeler, E. A., 1999 Functional Characterization of the *S. cerevisiae* Genome by Gene Deletion and Parallel Analysis. *Science* 285: 901-906.

Yvert, G., R. B. Brem, J. Whittle, J. M. Akey, E. Foss *et al.*, 2003 Trans-acting regulatory variation in *Saccharomyces cerevisiae* and the role of transcription factors. *Nat Genet* 35: 57-64.

Zhu, J., B. Zhang, E. N. Smith, B. Drees, R. B. Brem *et al.*, 2008 Integrating large-scale functional genomic data to dissect the complexity of yeast regulatory networks. *Nat Genet* 40: 854-861.

Figure 1

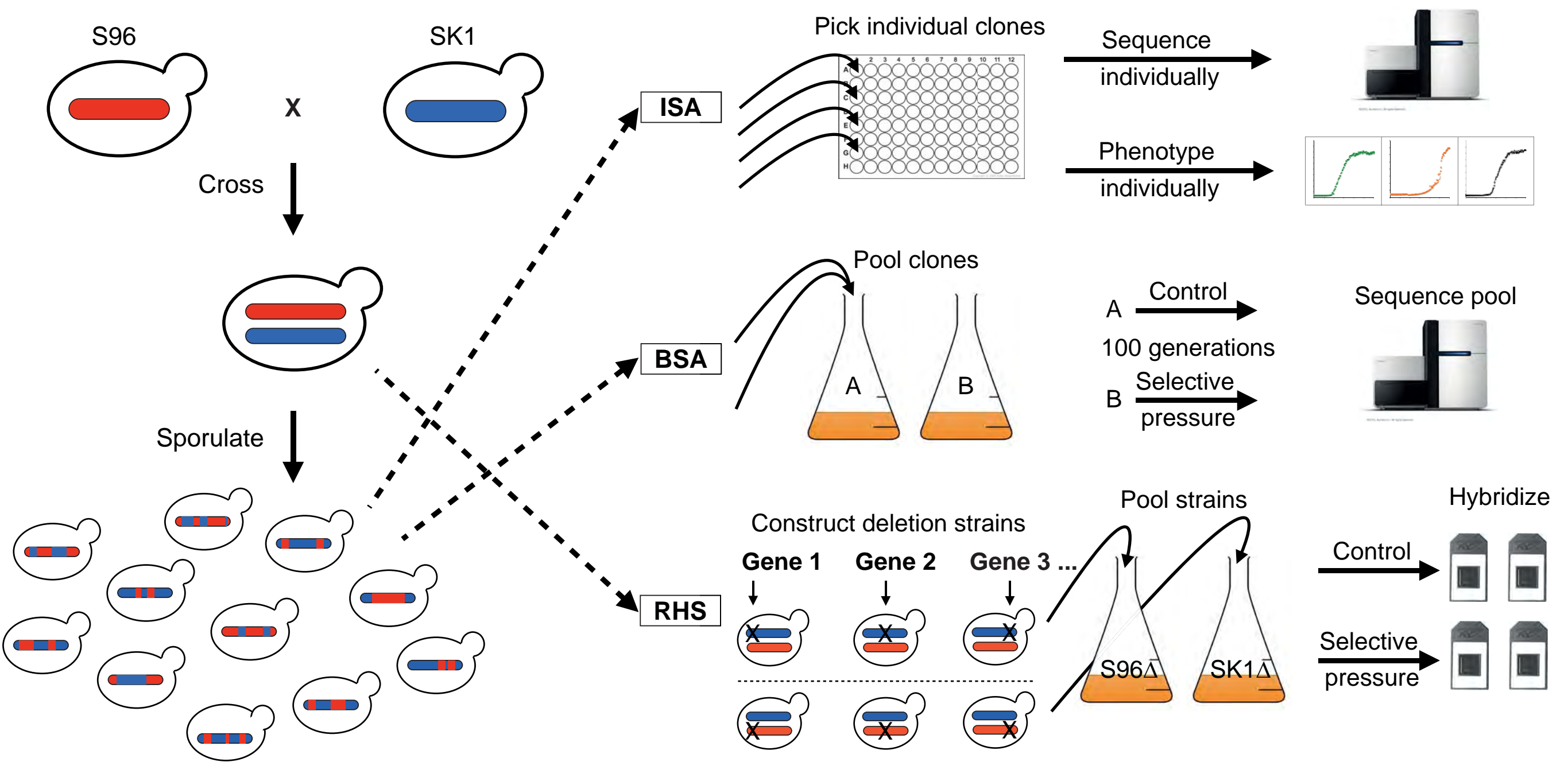


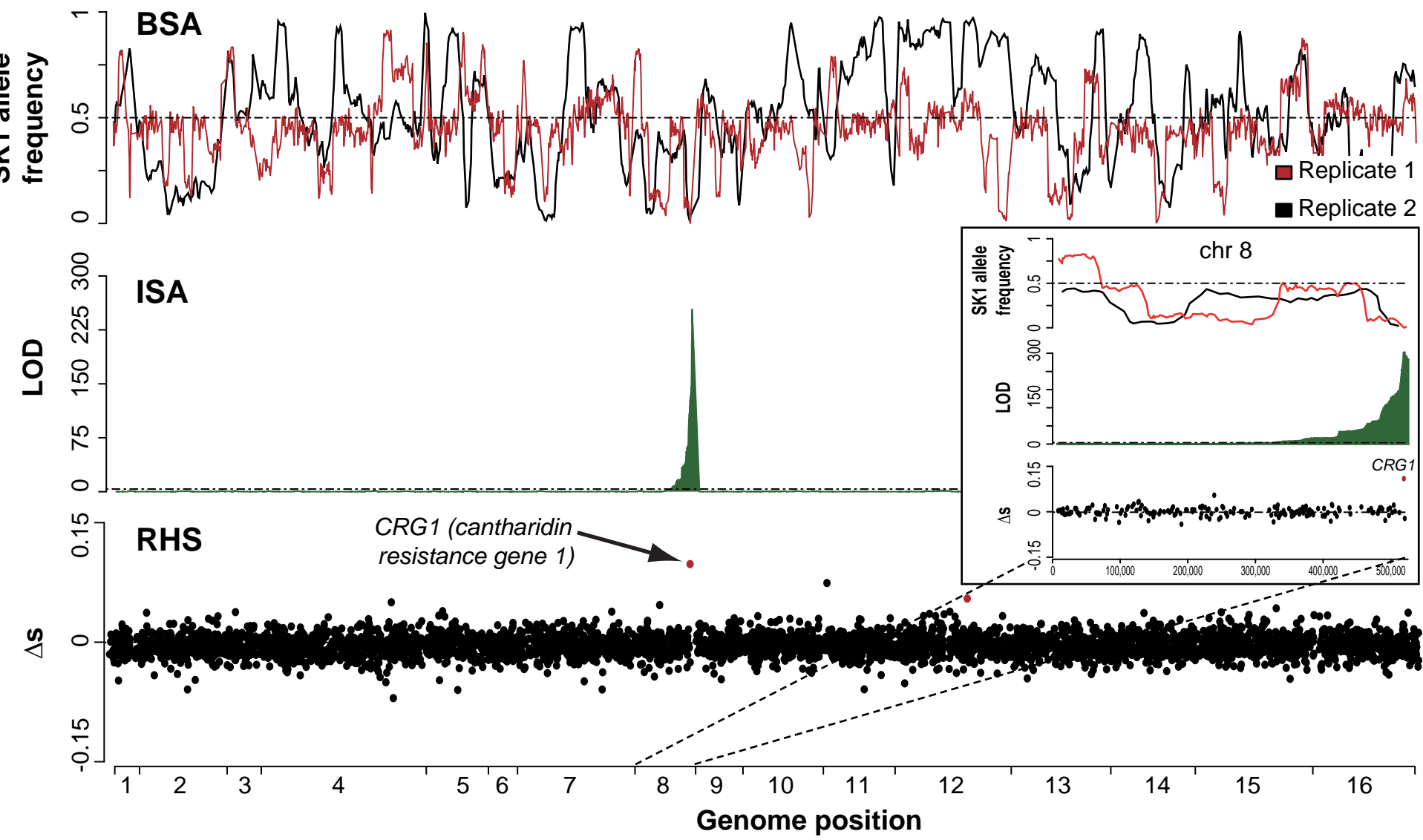
Figure 2

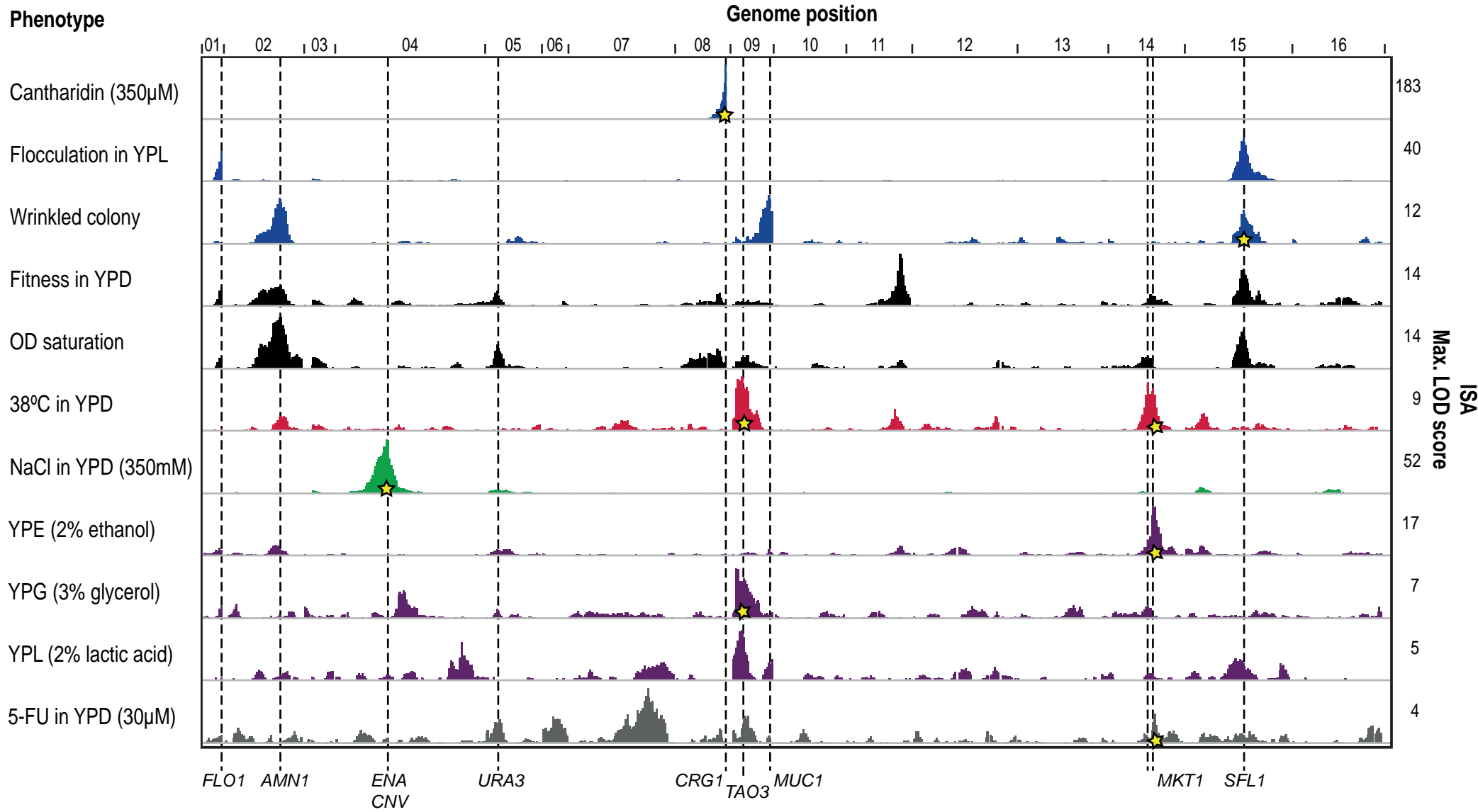
Figure 3

Figure 4

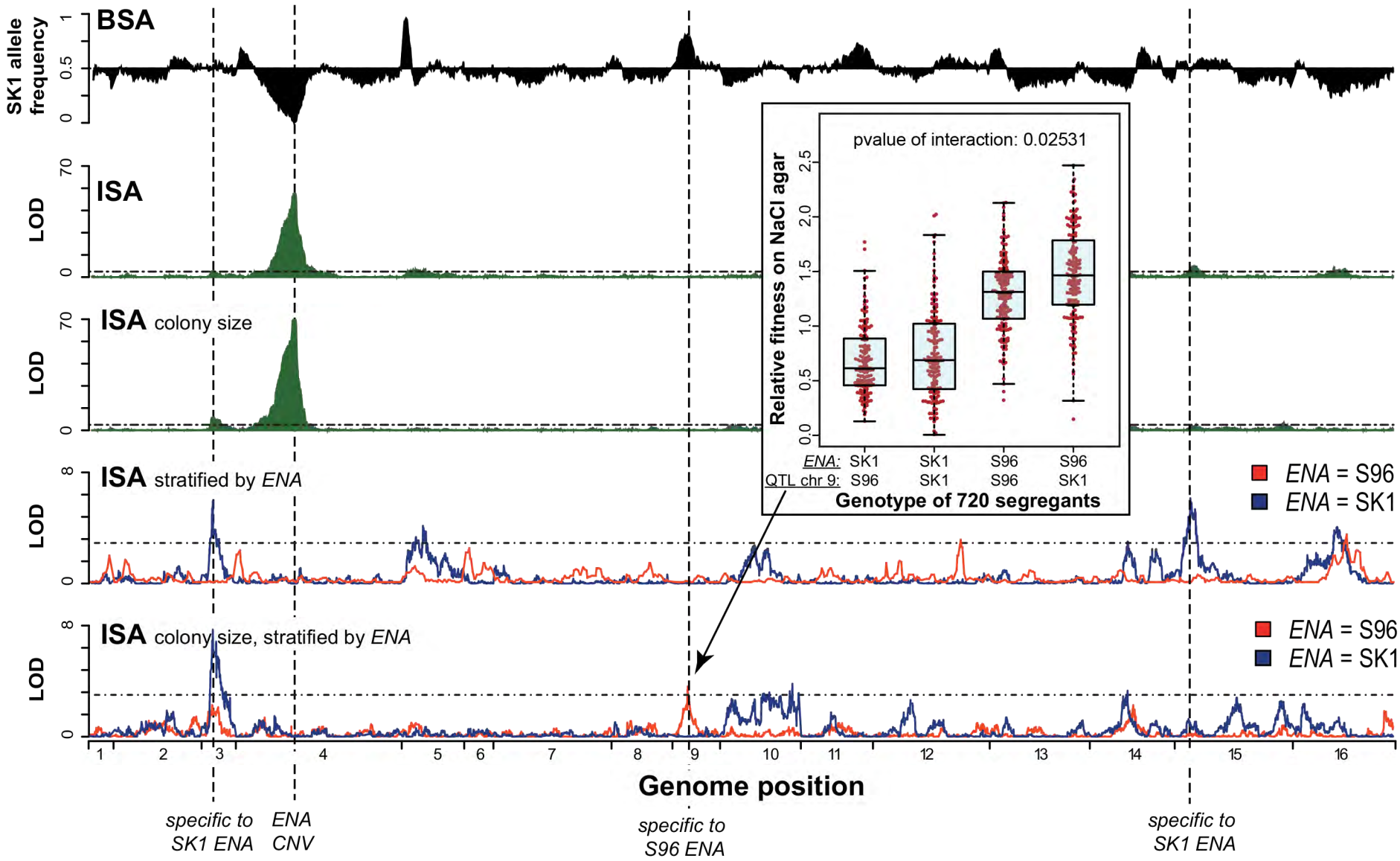


Figure 5